

DUPLICATE ALSO



Met O (APR) Turbulence and Diffusion Note No. 257

**Off-line Radiation Calculations Using an
LEM simulation of TOGA-COARE.
Part 2: Investigation of cloud water and
ice inhomogeneities**

by

J. C. Petch¹, S. Cusack² and J. M. Edwards²

12th July 1999

¹Atmospheric Processes Research

²Hadley Centre for Climate Research

Meteorological Office

London Road

Bracknell

Berks, RG12 2SZ

ORGS UKMO T

National Meteorological Library

FitzRoy Road, Exeter, Devon. EX1 3PB

This paper has not been published. Permission to quote from it should be obtained from the Head of Atmospheric Processes Research Division, Met O (APR), Meteorological Office, London Road, Bracknell, Berkshire, RG12 2SZ.

DUPLICATE ALSO



Met O (APR) Turbulence and Diffusion Note No. 257

**Off-line Radiation Calculations Using an
LEM simulation of TOGA-COARE.
Part 2: Investigation of cloud water and
ice inhomogeneities**

by

J. C. Petch¹, S. Cusack² and J. M. Edwards²

12th July 1999

¹Atmospheric Processes Research

²Hadley Centre for Climate Research

Meteorological Office

London Road

Bracknell

Berks, RG12 2SZ

This paper has not been published. Permission to quote from it should be obtained from the Head of Atmospheric Processes Research Division, Met O (APR), Meteorological Office, London Road, Bracknell, Berkshire, RG12 2SZ.

Off-line Radiation Calculations Using an LEM simulation of TOGA-COARE. Part 2: Investigation of cloud water and ice inhomogeneities

JON C. PETCH

Atmospheric Processes Research, Meteorological Office, Bracknell, Berks, UK

STEPHEN CUSACK AND JOHN M. EDWARDS

Climate Research, Meteorological Office, Bracknell, Berks, UK

July, 1999

ABSTRACT

Observations have shown that many types of clouds have horizontal inhomogeneity in their liquid and ice water contents. This variability is likely to be very important when considering the parametrization of the radiative properties of clouds in a General Circulation Model. In the work presented here, results from 2-D and 3-D Large Eddy Model simulations of a 5 day period of TOGA-COARE have been used to investigate the influence of horizontal variations of in-cloud hydrometeor contents on the UK Meteorological Office Unified Model radiation scheme. The effect of cloud inhomogeneities on top of atmosphere irradiances and in-cloud heating rates were shown to be large in both the solar and infra-red spectrum. Two different parametrization schemes were tested to represent the effects of in-cloud variability in the Unified Model radiation scheme. Both parametrization schemes improved the radiation calculations but neither was conclusively better than the other. Tests of the assumed hydrometeor distributions used in the more complex scheme showed that they were inconsistent with the hydrometeor distributions produced by the Large Eddy Model.

1. Introduction

Many types of clouds, including those described as stratiform, exhibit considerable horizontal variability on the scales less than typical General Circulation Model (GCM) grid boxes (e.g. Hignett and Taylor, 1996). Often, this sub-grid scale variability is represented in GCMs by having cloudy and cloud free regions in the model. Typically, no allowances are made for variability of in-cloud water and ice contents which can have a strong influence on the averaged radiative properties of clouds over a grid box.

There are two main reasons why cloud inhomogeneities can influence domain averaged radiative properties calculated in a typical GCM. Firstly, by using a domain averaged cloud field, no allowance can be made for the horizontal transport of photons, thus passing through

regions of different cloudiness. This is particularly important at high zenith angles where a cloud can effectively cast a large horizontal shadow. This effect would be missed by any domain average calculation or by any model which uses plane parallel radiative transfer calculations such as a two stream scheme. This type of approximation is referred to as the Independent Pixel Approximation (IPA) and the bias introduced through neglecting cloud inhomogeneities and the horizontal transport of photons is often referred to as the plane parallel bias. The influence of the IPA is not the focus of this study but research into this area is planned to be carried out by the radiation group in APR (Francis, personal communication) and requires the use of a multi-stream or Monte-Carlo radiation code. It is possible that on the scales of a GCM grid box over periods of a day that this effect may not be

important.

The second influence of the cloud inhomogeneities on radiative transfer is caused by the non-linear dependence of a clouds optical properties on cloud water and ice contents. This can introduce a systematic bias to the radiative properties of a cloud because the averaged cloud properties will always over estimate the optical thickness of a cloud. Unlike the plane parallel bias, this systematic bias is likely to have a large influence on the scales of a GCM grid box. This problem can be investigated with the use of a plane parallel radiation scheme (i.e. using the IPA) and is the focus of this study.

Several recent studies have used either satellite data, microwave soundings or in-situ observations to investigate the extent of variability of in-cloud water contents and the influence of cloud inhomogeneities on radiative transfer. Barker (1996) and Barker et al. (1996) used satellite observations of marine stratocumulus with a pixel size of 20-50 m to develop and test a parametrization of cloud inhomogeneities for use in GCMs. Oreopoulos and Davies (1998) used satellite data from a larger domain (9° to 45°N ; 19° to 58°W) but a lower resolution (1.1 km pixel size) to study the influence of the plane parallel bias on the top of atmosphere (TOA) solar irradiances in GCMs. They found that the bias could be as large as 30 Wm^{-2} and often GCMs would tune their treatment of cloud water content to compensate this bias.

Cahalen et al. (1994) and Cahalen et al. (1995) used data from an upward looking microwave radiometer during ASTEX and FIRE to study variability of in-cloud water contents of stratocumulus and fair weather cumulus and the corresponding plane parallel bias. They found that the largest biases in albedo were at high zenith angles but there was little energy around this time. They also found a sensitivity to the cloud threshold value used by their instruments. A typical bias in albedo was 0.1 which they believed was caused half by the in-cloud

inhomogeneities and half by the cloud field being broken.

The above studies have shown that the horizontal variability of cloud water has a major impact on radiative transfer calculations. Therefore, for a GCM to represent the radiative properties of clouds reasonably it needs information on the distribution of water contents within a grid box as well as a cloud fraction and the average water content. It should be stressed that these previous studies all used observations of stratocumulus and cumulus clouds in mid latitudes. Clearly geographical region, and more importantly cloud type will have a large influence on the effect of the cloud inhomogeneities. To the authors' knowledge, no studies into the influence of cloud inhomogeneities in ice clouds or mixed phase clouds have been carried out. The work presented in this paper will focus on the influence of cloud inhomogeneities in tropical deep convection.

Petch and Edwards (1999), hereafter part 1, described some experiments where output from the UK Meteorological Office Large Eddy Model (LEM; Mason, 1989; 1994) was used to test the cloud overlap assumption in The UK Meteorological Office Unified Model (UM; Cullen, 1993). In this companion paper we use the same method to investigate the influence of the variability of in-cloud water contents and test two parametrizations schemes to represent cloud inhomogeneities which could be included in the UM radiation scheme (Edwards and Slingo, 1996). As stated earlier, this work uses a plane parallel radiation scheme so the influence of the IPA is not considered. What is studied is the effect of the non linear dependence of a clouds radiative properties on cloud water and ice contents. As was the case with part 1, the LEM simulation used a horizontal grid length of 2 km so details of inhomogeneities at length scales less than this will not be captured. A further point to note is that the UM radiation scheme allows for two cloud types besides the clear sky. There is large scale cloud produced by a resolved moisture structure, and convective cloud produced by the convection scheme. As these

clouds can have different radiative properties, the UM effectively allows for some inhomogeneity in a very crude manner.

Section 2 describes the relevant features of the LEM simulation not mentioned in part 1; this includes the diagnostic partitioning of the cloud into two types. Section 3 discusses the influence of the inhomogeneities and section 4 describes and shows the influence of two possible parametrization schemes. Section 5 discusses the importance of the two cloud types in the UM and how the parametrization schemes can be applied to this. Section 6 looks at the assumed hydrometeor distributions of the Barker (1996) scheme and compares these to those produced by the LEM. A summary and conclusions are given in section 7.

2. The LEM Simulation

As detailed in part 1, the LEM was forced with large scale motion from a 5 day period (20-25th December 1992) of TOGA-COARE (Tropical Ocean Global Atmosphere Couple Ocean Atmosphere Response Experiment; Webster and Lucas, 1992; Krueger and Lazarus, 1998). Results from radiative transfer calculations on datasets from a 2-D (Petch, 1999) and 3-D simulation (M. E. B. Gray, personal communication) will be shown. In part 1, radiative transfer calculations were performed on the 2-D datasets at 0Z on the 22nd (day 2), 23rd (day 3), 24th (day 4) and 25th December (day 5). The work presented here will focus mainly on days 2, 3 and 5 because there was very little cloud on day 4 so the effects of inhomogeneities are small.

All the radiative transfer calculations are done with a fixed solar zenith angle of 60° and an insolation of 1411 Wm^{-2} . Precipitation sized hydrometeors are included in the radiation scheme using the method shown in part 1. Figure 1 shows linear and log contour plots of hydrometeor contents (including scaled precipitation) for days 2, 3, 4 and 5 of the 2-D simulation. This gives some indication of the variation in hydrometeor contents within the cloud. One point to note is that the lowest contour interval

in the linear plot is 0.05 g kg^{-1} whereas in the log plot it is $10^{-3} \text{ g kg}^{-1}$ which is the critical value for a model point to be defined as 'cloudy'. This implies that on days 2 and 5 there are large areas of cloud with low water contents. This is likely to be significant for the influence of cloud inhomogeneities and is discussed further in section 6.

To make some single column model calculations consistent with the UM, the clouds must be categorized into convective and large scale. There are various ways this can be done (e.g. using a critical updraught velocity) but a simple method which is likely to be most consistent with the UM is to use a 'critical mixing ratio' (CMR). The CMR is defined such that any point with a hydrometeor mixing ratio above this contains convective cloud and any 'cloudy' point with a mixing ratio below this contains large scale cloud. The threshold for precipitation in the UM convection scheme is 1 g kg^{-1} so this could be used as a sensible value for the CMR. However, in recent versions of the UM this is then scaled by an 'updraught factor' for use in the radiation scheme (Gregory, 1998). The updraught factor is currently 0.12 and therefore, for the work presented in this paper the CMR used is 0.12 g kg^{-1} .

Figure 2 shows the convective and large scale cloud fraction produced by the 2-D and 3-D LEM simulations from days 2, 3 and 5. It can be seen from these plots that the convective cloud has a relatively large cloud fraction (as large as 0.4 on days 3 and 5). The reason for this is that the convective cloud in the UM is defined such that it includes some of the detrained anvil as well as the convective core. Another point to note from Figure 2 is that the 2-D and 3-D simulation have very similar cloud fractions, with the 3-D run having smoother profiles because it is the average of many more points.

3. The influence of Cloud Inhomogeneities on SCM Radiative Transfer

To investigate the importance of cloud inhomogeneities on radiative transfer we can compare

the domain averaged heating rates (LEM) with the single column (SCM) radiation calculations. The SCM calculation is a single calculation using domain averaged cloud water, cloud fraction, temperature and water vapour fields from the LEM. For the work described in this section we will use one cloud type in the SCM calculations as was done in part 1, therefore the convective and large scale cloud (Figure 2) are combined; section 5 discusses the influence of separating these two cloud types.

To investigate the influence of cloud inhomogeneity on the single column calculations it is necessary to separate out this effect from other potential causes of differences between domain average and single column heating rates. Other causes may be variations in the horizontal distributions of water vapour or the cloud overlap assumptions used in the SCM (see part 1). The influence of cloud inhomogeneity can be isolated by doing full radiative transfer calculations on an LEM dataset which has had the cloud 'homogenized'. This involves changing the cloud water and ice contents on every 'cloudy' grid point in the LEM dataset to be the in-cloud mean value. This technique does not change the domain averaged properties of the cloud and was used in part 1 to remove the influence of cloud inhomogeneities while investigating the overlap problem.

Figure 3 shows the solar and infra-red heating rates from days 2, 3 and 5 of the 2-D LEM simulation. It can be seen that on all 3 days shown, the solar and infra-red heating rates from the SCM calculation differ significantly from the LEM. However, when the cloud is homogenized in the LEM dataset (HOM), the heating rates are very close to the SCM calculations. There are some notable but relatively small difference between the HOM and LEM results in the infra-red which are due mainly to the overlap assumptions used and have been discussed in part 1 of this work.

Figure 4 shows the same as Figure 3, only datasets from the 3-D LEM simulation have been used. It can be seen that the heating rates

are generally similar to those of the 2-D dataset, although the infra-red heating rates on day 2 are notably smaller for the 3-D simulation. This is due to the smaller cloud fraction on this day in the 3-D LEM simulation as can be seen in Figure 2. The 3-D dataset shows the same features as the 2-D datasets when considering the effects of the cloud inhomogeneities. It is clear that whether a 2-D or 3-D LEM simulation is used, the cloud inhomogeneity is very important for the radiative heating rates in both the solar and infra-red. The influence is largest when there is a lot of cloud i.e. days 3 and 5. In these cases the inhomogeneity is by far the most significant reason for differences between the SCM calculation and the domain averaged heating rates from the LEM. This is different from the influence of the overlap problem discussed in part 1 which was not important with a cloud fraction of unity.

Figure 5 is a bar graph showing the Outgoing Longwave Radiation (OLR) for days 2, 3 and 5 of all the 3-D (top) and 2-D (bottom) radiative calculations described in this paper. Focusing on the left three bars we can see the influence of the inhomogeneity on the OLR. Clearly for both the 3-D and 2-D runs, the HOM and SCM calculations are very similar (within 3 Wm^{-2}). However, results from the LEM which includes the inhomogeneity differs by up to 40 Wm^{-2} from the SCM or HOM results. This shows that the cloud inhomogeneity can account for almost all the difference in OLR between the SCM and LEM calculations. In part 1 it was shown that the overlap assumption had a smaller influence than this on the OLR, particularly in thick cloud cases such as days 3 and 5.

Figure 6 is a bar graph for the same experiments as Figure 5 only showing the TOA net downward solar irradiance. Again, by focusing on the left three bars we can see the influence of the inhomogeneity on this field. Understanding these bar graphs is somewhat more difficult than the OLR as there are significant differences between the SCM and the HOM for all days. The differences suggests that biases due to other things such as the overlap are smaller but of a similar order to the influence of the

inhomogeneity. This is consistent with results from part 1 which found the choice of cloud overlap assumption to have a large impact on the TOA net downward solar irradiance.

The differences between the HOM and LEM calculations show the influence of the inhomogeneity on the downward solar irradiance. On all days in both 2-D and 3-D, it can be seen that the net downward irradiance for the LEM calculation is between 40 and 80 Wm^{-2} greater (less is reflected) than when the cloud is homogenized; this implies that we can expect the SCM to underestimate this by the same amount. However, this error is offset for the single column UM radiation calculation because it used the maximum-random overlap which tended to overestimate the net downward solar by between 20 and 40 Wm^{-2} . Therefore the SCM calculations are nearer the truth but for the wrong reasons. This is important when considering parametrizations which correct for cloud inhomogeneity because these should make the SCM calculations overestimate the net downward solar irradiance.

The difference between the influence of cloud inhomogeneities on the 2-D and 3-D calculations are small. It appears that the effects of inhomogeneities are smaller in the 2-D runs which could be expected given the far fewer grid points, but these differences are much smaller than the effects of inhomogeneities themselves. This finding is useful for groups wishing to investigate this type of problem without doing the computationally expensive 3-D LEM simulations. However, the rest of this paper will focus on full 3-D simulations because this is clearly the most realistic method of testing the importance of cloud inhomogeneities and potential methods of parametrization.

4. Testing Cloud Inhomogeneity Parametrization in the UM

In section 3 it was shown that cloud inhomogeneities had a large influence on infra-red and solar TOA irradiances and in-cloud heating rates. In this section we consider two different

parametrizations schemes which will allow for the radiative effects of cloud inhomogeneities in single column calculations. One method tested is a simple scheme used by Tiedtke (1995) which was based on the work of Cahalen et al. (1994). This scheme, hereafter referred to as PNT, reduces the optical thickness of a cloud by a factor 0.7 at all model levels.

The second scheme, hereafter referred to as BKR, is based on the work of Barker (1996) and Barker et al. (1996). The BKR scheme estimates the variability of cloud optical thickness in a grid box from parameters available in a typical GCM. This is done by assuming a normalized gamma distribution of optical thickness, which allows the mean and the standard deviation of this to specify the cloud inhomogeneities. Based on a series of satellite observations Barker et al. (1996) expressed the standard deviation of a cloud optical depth in terms of the cloud fraction. Using this information, an SCM can then describe the cloud distribution within a grid box.

To apply the BKR parametrization to the UM radiation scheme, a scaling factor is calculated on each level which is used to adjust the mean optical thickness. The scaling factor is estimated using an empirical relation between the mean and standard deviation of the cloud water content with the optical thickness of the cloud. For a given standard deviation, the scaling factor was calculated using a quartic fit based on off-line radiation calculations using a wide range of optical thickness and standard deviations of cloud water contents.

Figure 7 shows the influence of the two parametrizations on results from the 3-D LEM simulation for both the infra-red and solar spectrums. It is clear that neither schemes do very well in all cases but both do improve the heating rates in most cases. The PNT scheme appears to do better than the BKR scheme on days 3 and 5 in the solar region but it is not clear this is true for all days. It appears that in general, for the cases shown, the BKR scheme reduces the optical

depths of the cloud more than the PNT scheme but not uniformly through the cloud.

Comparing the 4th and 5th bars on Figures 5 and 6 we can see that the two parametrization schemes do improve the OLR and TOA net downward solar irradiance. The improvement to the OLR is clearly not enough. The best any scheme did was the BKR on day 2 but this still only increased the OLR by 20 Wm^{-2} when an increase of 40 Wm^{-2} was required to match the LEM result. On other days the BKR and PNT scheme increase the OLR by about 5 Wm^{-2} when an increase of about 20 Wm^{-2} is required to match the LEM result.

In the solar spectrum, the parametrizations (particularly BKR) appear at first to do a good job of representing the inhomogeneities. In particular, the TOA net downward solar irradiance for the BKR run is within 10 Wm^{-2} of the LEM. However, this is not as good as it might first appear because as stated earlier, the SCM already overestimated this by up to 40 Wm^{-2} so if the parametrization worked well the BKR and PNT calculations would be 40 Wm^{-2} bigger than the LEM result. It should be stressed that both parametrizations do improve the TOA fluxes but both could do better. Ideally both schemes need to reduce the optical thickness of the clouds by more, although as the heating rates showed, it is important what height in the cloud the adjustments are made.

5. Testing Cloud Inhomogeneity Parametrization in the UM with Two Cloud Types

In the section 2 we described how the UM uses two cloud types with different optical properties. Here we show how the BKR and PNT parametrization perform when two cloud types are included in the SCM calculation. The basic run without parametrizations referred to as UMA, will differ from the SCM run because by using two cloud types some very simple allowance for inhomogeneities are being made. The parametrization schemes can then be included in two ways, firstly they can be applied only to the large scale cloud; these calculations are referred

to as UMB and UMP for the Barker and Point 7 parametrizations respectively.

The heating rates for the UMB and UMP runs are not shown as the effect of including these schemes only in the large-scale cloud is relatively small. This can be seen in Figures 5 and 6 where the UMB and UMP are within 5 Wm^{-2} of the UMA for OLR and within 10 Wm^{-2} for the TOA net downward solar. Of more interest is what happens when a correction is also applied to the convective cloud, which is more likely to be inhomogeneous by nature. This adjustment is done differently for the two schemes. For the UMP case we simply multiply the optical depth of both cloud types by 0.7; this run is referred to as CVP. For the UMB, the convective clouds optical depth is multiplied by 0.5 at all levels. This is done because the Barker scheme was based on stratiform clouds but a value of 0.5 was suggested by Kogen et al. (1995) for convective clouds based on a modelling study.

The infra-red and solar heating rates for runs SCM, UMA, CVB and CVP are shown in Figure 8. Comparing the UMA with the SCM heating rates in Figure 7 shows the influence of using two cloud types in the UM radiation scheme. It can be seen that the two cloud types do improve the heating rates but the differences from the LEM are still large. The biggest improvements from using two cloud types (UMA) can be seen in the infra-red where the differences from LEM are halved on days 3 and 5. The OLR (Figure 5) for the UMA is between 5 and 10 Wm^{-2} greater than the standard SCM run for the 3 days shown. The TOA net downward solar (Figure 6) for the UMA differs by around 10 Wm^{-2} from the standard SCM run.

When the two parametrization schemes are applied to both cloud types (CVB and CVP), the heating rates (Figure 8) improve in both the solar and infra-red spectrum. By comparing with Figure 7, it can be seen that the parametrizations applied to both cloud types do significantly better than when they were applied to only one cloud type. In both the solar and infra-red the CVB and CVP match the LEM heating profiles

much better than the BKR and PNT. It is less clear which gives the best heating profiles between CVB and CVP. On all days in the solar spectrum the CVB scheme matches the LEM scheme best below 5 km. This suggests that it is representing the optical depth of the cloud better. However, through most of the depth of the cloud neither scheme does systematically better than the other at representing the LEM heating rate profile. This is also true in the infra-red spectrum where both schemes significantly improve the heating profile but neither scheme is clearly better.

Comparing the influence of the schemes on the TOA fields shows that the CVB scheme is having the largest impact on both the OLR and net downward solar irradiance. This can be seen in Figures 5 and 6 where the OLR is around 3 Wm^{-2} greater and the net downward solar is 20 Wm^{-2} greater with the CVB scheme than CVP scheme. The main reason that the CVB scheme changes the optical properties of the clouds more is that the convective clouds optical depth was multiplied by 0.5 in this scheme and by 0.7 in the CVP scheme. For the simulation shown, using the given method of partitioning clouds into convective and large scale, the optical properties of the convective clouds are very important.

The changes by both schemes to the TOA irradiances are smaller than required to match the LEM results. The OLR needs increasing by a further factor of 2 from the UMA result to come close to matching the LEM. The net downward solar should be over-estimated by between 20 and 40 Wm^{-2} when the schemes are applied but tend to only overestimate this by 10 Wm^{-2} . This means the schemes should increase the net downward solar by a further 30 to 50%.

6. Cloud Water Distributions Produced by the LEM

The BKR parametrization, taken from Baker (1996) and Barker et al. (1996), assumes a

normalized gamma distribution of cloud water (or optical depth) which is given by

$$p(\tau) = \frac{1}{\Gamma(v)} \left(\frac{v}{\bar{\tau}} \right)^v \bar{\tau}^{v-1} e^{-v\tau/\bar{\tau}}, \quad (1)$$

where $v = (\bar{\tau}/\sigma)^2$ in which $\bar{\tau}$ and σ are the mean and standard deviation of the cloud water or optical depth τ . The value of $\bar{\tau}$ is known from the large scale model but what is not known is the standard deviation. This is given in terms of v by the empirical relation with cloud fraction, A_c ,

$$v \approx \frac{0.0284e^{4.4A_c}}{A_c - 0.0284e^{4.4A_c}(1 - A_c)}. \quad (2)$$

Some limits on the values of v discussed in Barker et al (1996) are also used in this work.

The gamma distribution and the empirical relationship with the cloud fraction can be tested using the LEM results directly. By taking 1 km vertical averages in the LEM we can calculate the mean cloud water content, the standard deviation and the cloud fraction. This allows us to look at the actual distribution of cloud water in the horizontal and compare with that assumed by the parametrization. Figure 9 shows the normalized distribution of cloud water at various heights for day 3 from the 3-D LEM simulation. The top plot is for all cloudy points and the bottom plot is for large scale cloudy point only. The dashed line is the normalized gamma distribution given by Eqn 1 using the observed standard deviation and the solid line is the distribution using the empirical relationship to cloud fraction given in Eqn 2.

From Figure 9 it can be seen that the gamma distribution can fit the distribution seen in the LEM if the correct values of v are used. Using the values of v taken from the LEM (dashed lines), the fit to the actual distribution is reasonable bearing in mind that the vertical axis uses a log scale. However, if the empirical value of v

is used then the approximation to the actual distribution is very poor. The distributions in the LEM have much larger frequencies at low water contents than that produced by the BKR scheme. This is true for all cloud types [top plot] (as was applied in Section 4) and large scale cloud [bottom plot] (as used in Section 5). Plots of distributions at several other times during the LEM simulation (not shown here) also found the approximation shown in Eqn 2 not to be representative of the LEM results. In each case the frequencies of low water contents were underestimated. This could be expected because the work of Barker (1996) was derived from observations of stratocumulus and not deep tropical convection simulated here.

7. Conclusions

Results have been presented which compare domain average radiative heating rates from an LEM with heating rates calculated using the domain averaged water vapour, temperature and cloud fields. Also shown have been TOA irradiances in the infra-red and solar spectrum from the same calculations. This allowed us to investigate the errors associated with single column (SCM) radiation calculations typical of those used in GCM simulations. The following limitations of this work should be made clear:

- 1) The LEM had a horizontal grid length of 2 km and any variation of in-cloud water contents on scales smaller than this was not represented.
- 2) The LEM uses a plane parallel radiation scheme so the influence of the horizontal transport of photons from one LEM grid box to the next is not considered.
- 3) The SCM calculations used the same vertical grid as the LEM. This may not be representative of many GCM vertical grids but did keep the SCM and LEM calculations more consistent with each other.
- 4) This study was confined to convection in the Tropical West Pacific and different cloud types

may give significantly different answers. However, the methodology used in the study could easily be expanded for all regions and cloud types.

A technique of 'homogenizing' the cloud was shown to be very useful in diagnosing the effects of horizontal variability of in-cloud water contents on SCM radiation calculations. By using this 'homogenized' cloud field in the LEM it was clearly shown that the cloud inhomogeneities were the dominant reason for differences between the LEM domain averaged radiative transfer and results from the SCM. It should be made clear that on the scale of a GCM grid box the inhomogeneity may not only be associated with a single cloud but a contribution may come from having several different clouds with a range of water contents.

Some other differences not related to cloud inhomogeneities were seen in the LEM and SCM radiation fields. In particular the TOA net solar irradiance and the infra-red heating rates below the cloud base differed even when the cloud was homogenized, but these differences were still significantly smaller than the effects of in-cloud inhomogeneities. Some of these other differences were attributed to the choice of cloud overlap assumptions discussed in part 1 (Petch et al., 1999). The cause of the systematic overestimation TOA net downward solar irradiance is less clear and requires further investigation but may well also be related to the cloud overlap scheme.

Given that cloud inhomogeneity was the biggest reason for differences between LEM and SCM calculations, two different parametrization schemes were tested which aimed to represent this. The first [BKR] was based on the work of Barker (1996) and used an empirical relationship between sub-grid distributions of cloud water in the SCM and a large scale cloud fraction. The other scheme [PNT] was used by Tiedtke (1996) in a GCM and is based on the work of Cahalen et al. (1994). This simpler scheme multiplies the optical depth of the cloud at all model levels by 0.7. Results showed that both schemes

improved the heating rates and TOA irradiances but neither scheme was conclusively better than the other. In both cases the total optical depth of the clouds needed reducing further to change the TOA irradiances by the correct amount.

It was pointed out that some GCMs such as the UK Meteorological Office Unified Model (UM) have two cloud types which can have different optical properties. This crude method of allowing inhomogeneity was shown to improve the SCM calculations by a small amount but falls a long way short of allowing for the full effect of the cloud inhomogeneities. The cloud in the LEM was separated into convective and large-scale using a Critical Mixing Ratio (CMR) of 0.12 g kg^{-1} .

When the parametrizations were tested by applying them to only the large scale cloud, their impact was small; this was because the convective cloud had a relatively large cloud fraction as it also included anvils detrained from the convection. For this reason a further adjustment was applied to the convective cloud on both schemes. For the BKR scheme, the convective cloud optical depth was multiplied by 0.5 at all levels; this was based on Kogen et al. (1995). For the PNT scheme the convective cloud optical depth was multiplied by 0.7 to be consistent with the large scale cloud. When these corrections were applied the heating profiles and TOA irradiances were much closer to the LEM but again neither method could be said to be better than the other. As was the case with only one cloud type the total optical depth of the clouds needed reducing further to change the TOA irradiances by the correct amount.

The distributions assumed by the BKR scheme were compared to actual distributions seen in the LEM. This showed that although the gamma distribution could fit the LEM data if the correct parameters were used, the empirical relationship between cloud fraction and sub-grid scale variability of cloud water was not relevant for deep convection in the tropics. Given the poor results from the empirical relation, there is no good reasons for using the BKR scheme globally in the

UM. It is possible it could be applied to stratocumulus cloud only but this should be investigated further. A further problem with the BKR scheme is that the method it uses to represent inhomogeneities makes the scheme dependent on the vertical resolution of the model. One feature of the BKR scheme which is of importance, particularly when considering the influence on climate experiments, is that it does have a spectral dependence; this is not considered by the PNT scheme.

Cloud inhomogeneities on scales between 2 km and 200 km have been shown to be very important for radiative transfer calculations. A possible method of parametrization considered in this work is to multiply cloud optical depths by a factor of 0.7. This was shown to always improved results and given current knowledge is likely to be the best method to represent cloud inhomogeneity globally. For the work shown here the factor of 0.7 tended to reduce optical depths by too little so a smaller factor could be considered. Given that the effects of inhomogeneities have been shown to be larger in convective clouds (Kogen et al., 1995) a possibility could be to use 0.7 for large-scale cloud and 0.5 for convective cloud. A further consideration should be to make the scaling factor a function of spectral region. Schemes such as this should be tested in a range of cloud types using the methodology described in this work.

Acknowledgments

We would like to thank Mike Gray who provided some of the 3-D LEM datasets used in this work. JP would also like to thank Steve Derbyshire and Julie Gregory for some useful discussions during this work. The development of the radiation code was supported by DETR under contract PEC/D 7/12/37.

8. References

- Barker H. W., 1996: A parameterization for computing grid-averaged solar fluxes for inhomogeneous marine boundary layer clouds. Part 1: Methodology and Homogeneous Biases. *J. Atmos. Sci.*, **53**, 2289-2303
- Barker, H.W., B.A. Wielicki and L. Parker, 1996: A parameterization for computing grid-averaged solar fluxes for inhomogeneous marine boundary layer clouds. Part II: validation using satellite data. *J. Atmos. Sci.*, **53**, 2304-2316
- Cahalan, R. F., W. Ridgway, W. J. Wiscombe and T. L. Bell, 1994: The albedo of stratocumulus clouds. *J. Atmos. Sci.*, **51**, 2434-2455
- Cahalan, R. F., D. Silberstein and J. B. Snider, 1995: Liquid water path and plane-parallel albedo bias during ASTEX. *J. Atmos. Sci.*, **52**, 3002-3012
- Cullen, M. J. P., 1993: The unified forecast/climate model. *Meteorological Magazine (U.K.)*, **142**, No. 1449 81-94
- Edwards J. M. and A. Slingo, 1996: Studies with a flexible new radiation code I: Choosing a configuration for a large scale model. *Q. J. R. Meteorol. Soc.*, **122**, 689-719
- Gregory, J. M., 1998: Representation of radiative effects of convective anvils. *Report on metweb*:http://www-hc/~hadjx/anv_mar98.ps.gz
- Hignett P. and J. P. Taylor, 1996: The radiative properties of inhomogeneous boundary layer cloud: Observations and modelling. *Q. J. R. Meteorol. Soc.*, **122**, 1341-1364
- Kogan, Z.N., D.K. Lilly, Y.L. Kogan and V. Filyushkin, 1995: Evaluation of radiative parameterizations using an explicit cloud microphysical model. *Atmos. Res.*, **35**, 157-172
- Krueger S. K. and S. M. Lazarus, 1998: Inter-comparison of multi-day simulations of convection during TOGA COARE with several cloud-resolving and single-column models. *Proceedings of the CLIVAR/GEWEX COARE98 Conference, Boulder, CO*. 351-352.
- Mason, P. J., 1989: Large-eddy simulation of the convective atmospheric boundary layer. *J. Atmos. Sci.*, **46**, 1492-1516
- Mason, P. J., 1994: Large-eddy simulation: A critical review of the technique. *Q. J. R. Meteorol. Soc.*, **120**, 1-26
- Oreopoulos L. and R. Davies, 1998: Plane parallel albedo biases from satellite observations. Part 1: Dependence on resolution and other factors. *J. Climate*, **11**, 919-932
- Petch J. C., 1999: The influence of radiation on 2-D LEM simulations of a 5 day period from TOGA-COARE. *Internal report*. In preparation.
- Petch J. C. and J. M. Edwards, 1999: Off-line radiation calculations using an LEM simulation of TOGA-COARE. Part 1: Investigation of the cloud overlap assumption used in the UM. *Atmospheric Processes Research, TDN 254*, 15 pp [Available from APR, UK Met Office, Bracknell, Berkshire]
- Slingo A. and H. M. Schrecker, 1982: On the shortwave radiative properties of stratiform water clouds. *Q. J. R. Meteorol. Soc.*, **108**, 1145-1178
- Tiedtke M., 1996: An extension of cloud-radiation parametrization in the ECMWF model: The representation of subgrid-scale variations of optical depth. *Mon. Weather Rev.*, **124**, 745-750
- Webster P. J. and R. Lucas, 1992: TOGA-COARE: The Coupled Ocean Atmosphere Response Experiment. *Bull. Amer. Meteor. Sci.*, **73**, 1377-1416

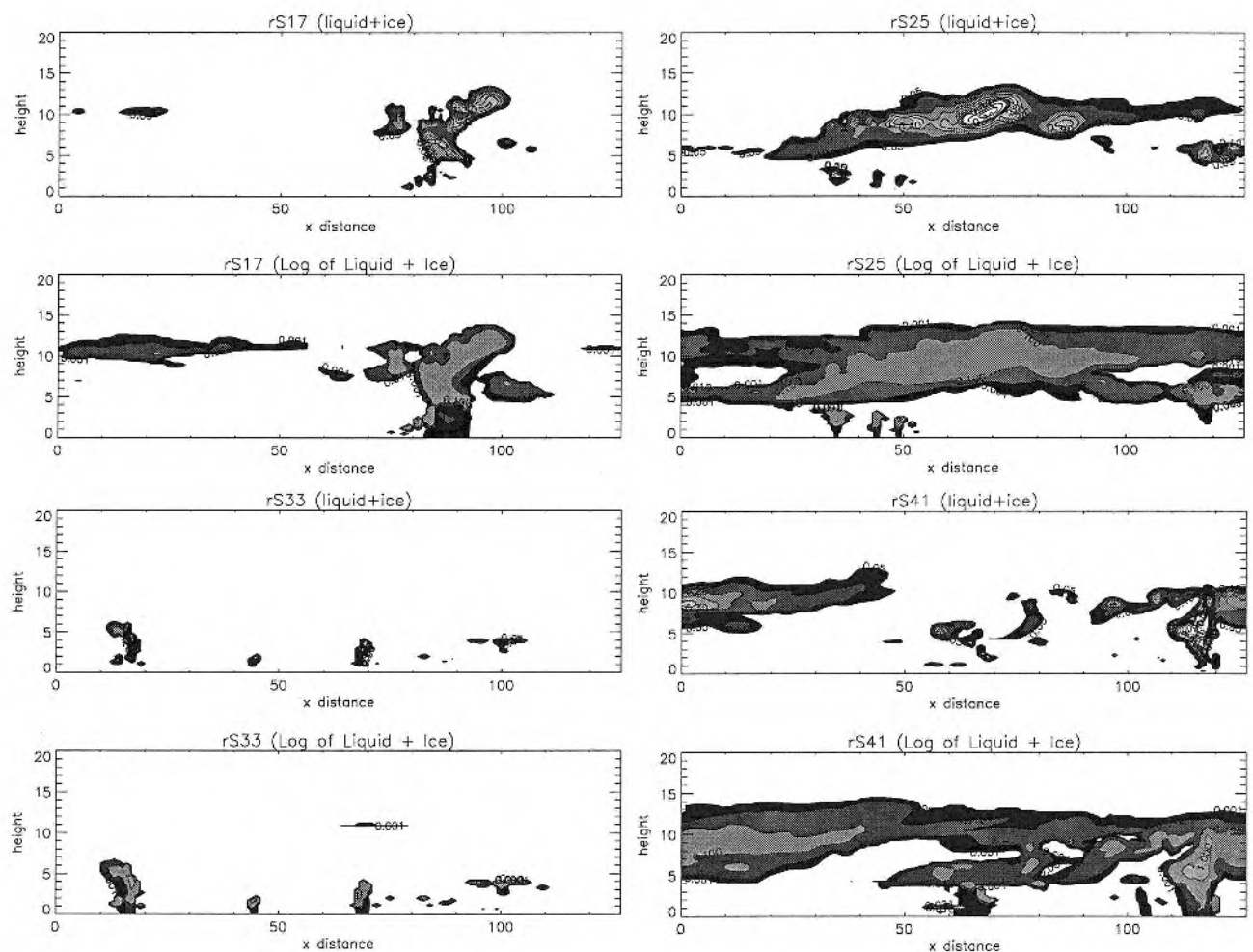


Figure1: Contour plots of total cloud water content (including scaled precipitation sized hydrometeors) from days 2 (S17), 3 (S25) 4 (S33) and 5 (S41) of the 2-D LEM simulation. The linear plot has a contour interval of 0.05 and the log plot has contours of 0.001, 0.01, 0.1 and 1 g kg⁻¹. The x distance values are in model grid points (2 km) and height is in km.

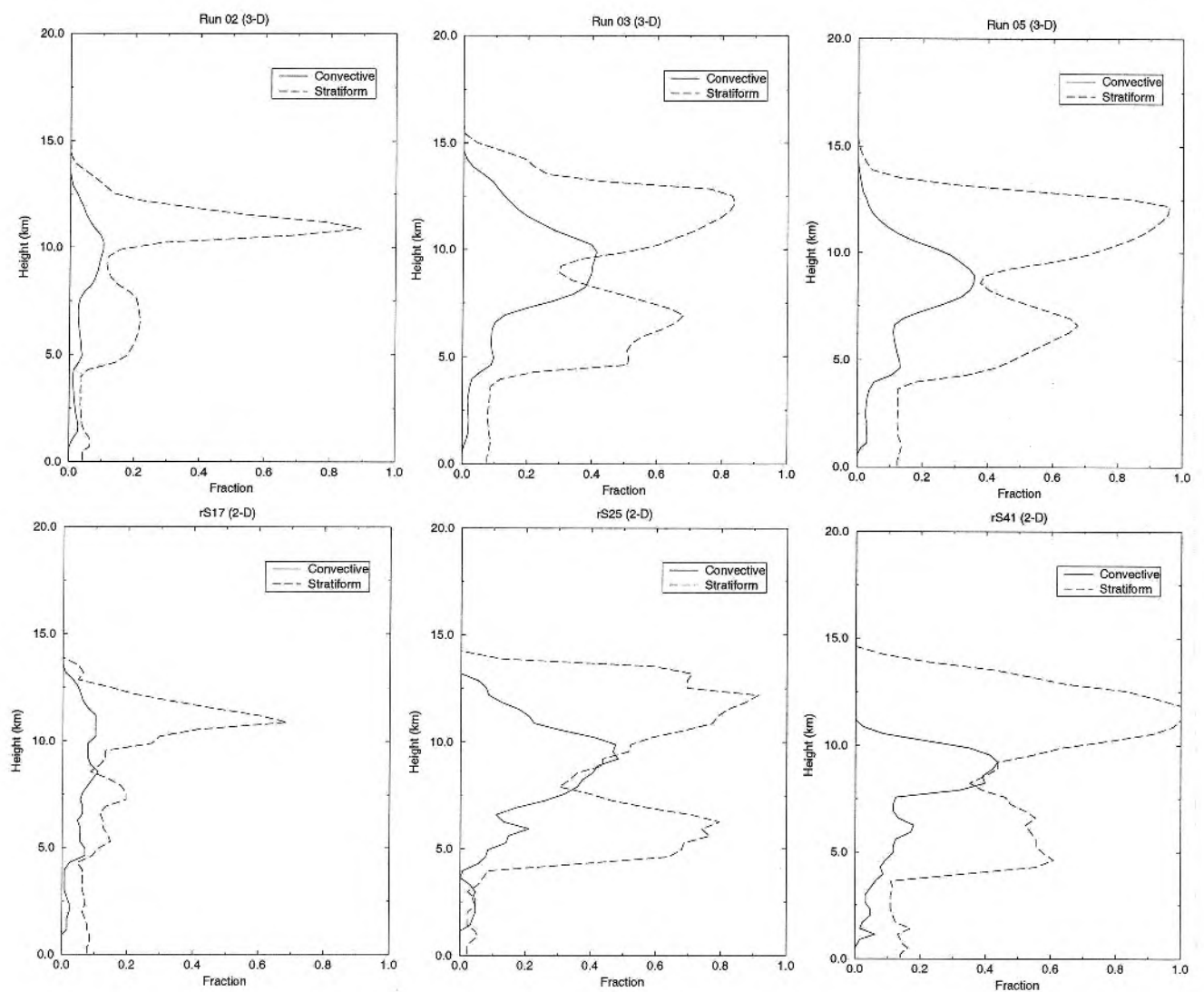


Figure 2: Large scale and convective cloud fractions from days 2, 3 and 5 of the the 3-D simulation (top row; run 02, run 03; run 05) and the 2-D simulation (bottom row; rS17; rS25; rS41). Shown are fractions where convective clouds are defined to have water contents greater than 0.12 gkg^{-1} .

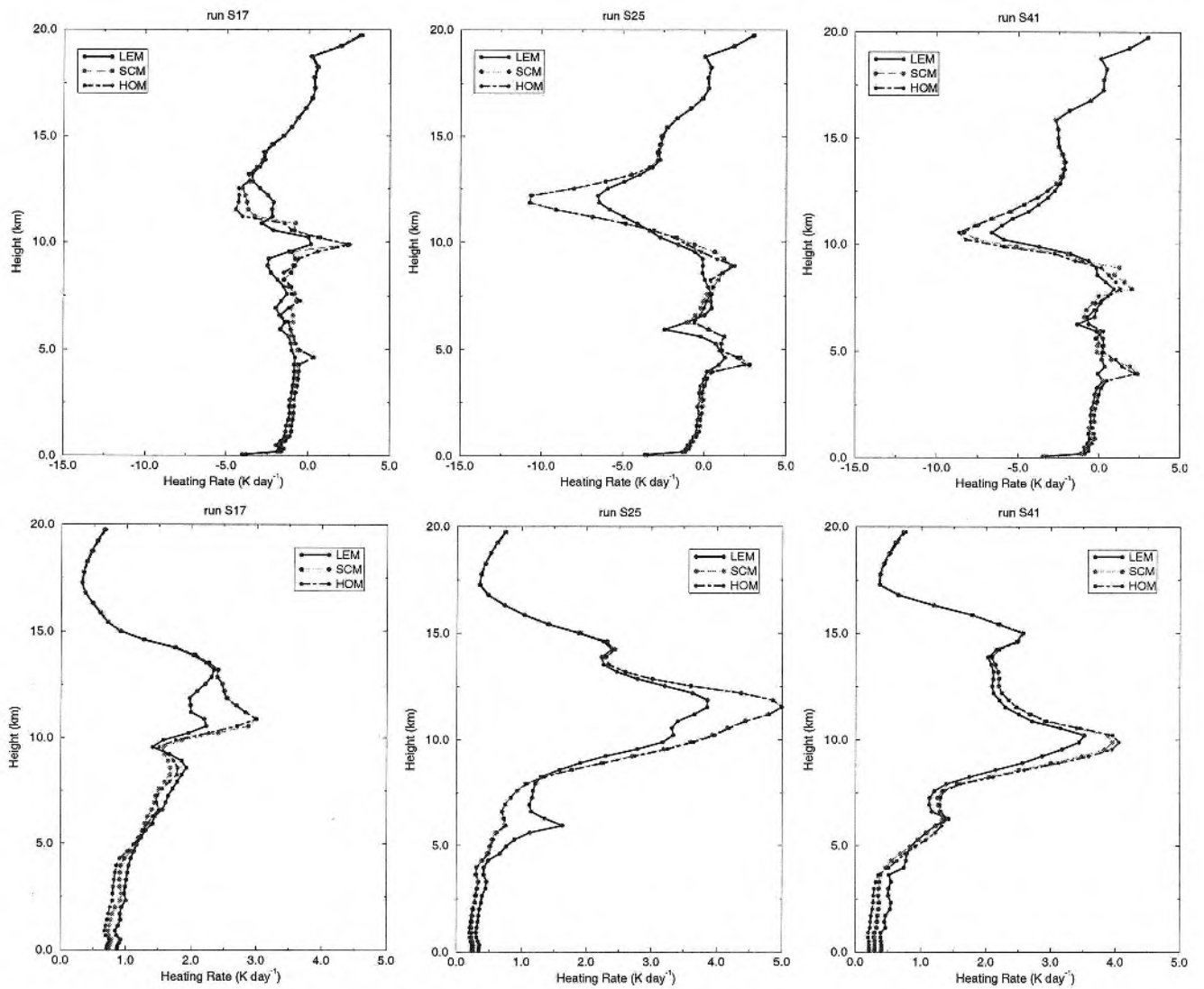


Figure 3: Infra-red (upper) and solar (lower) heating rates from days 2 (S17), 3 (S25) and 5 (S41). Shown are results from the 2-D LEM, from single column calculations [SCM] and from the 2-D LEM using homogeneous cloud [HOM].

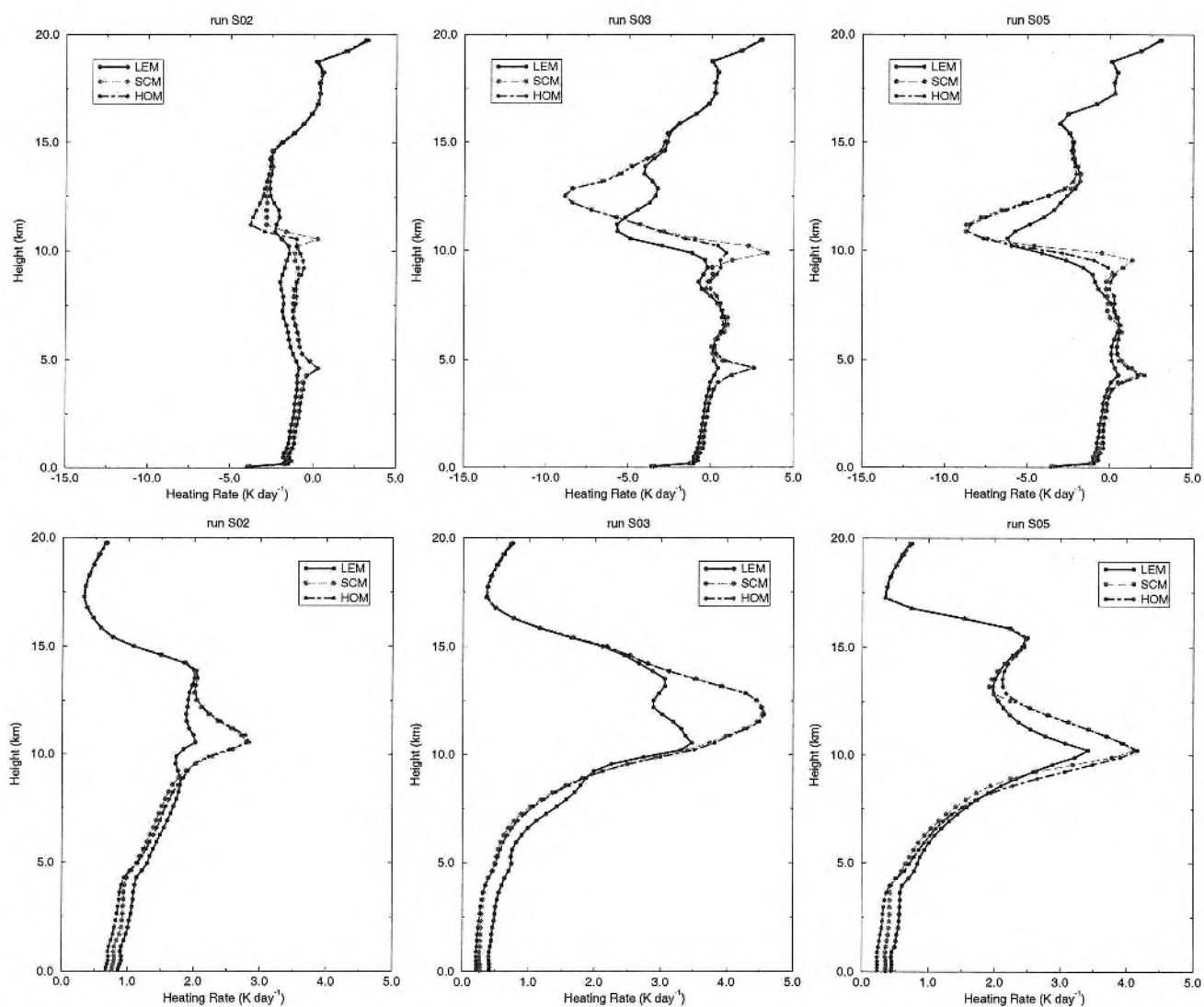
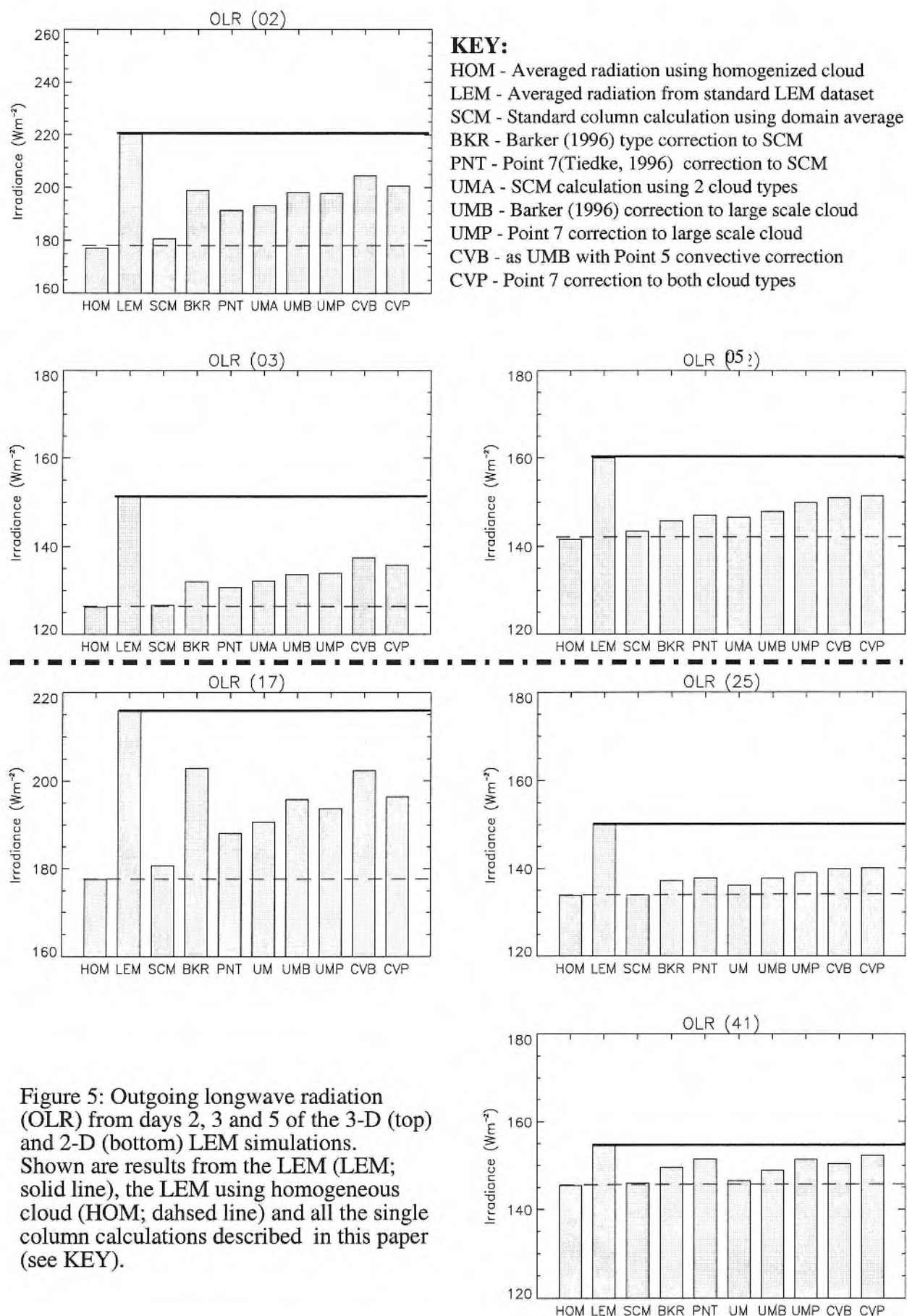
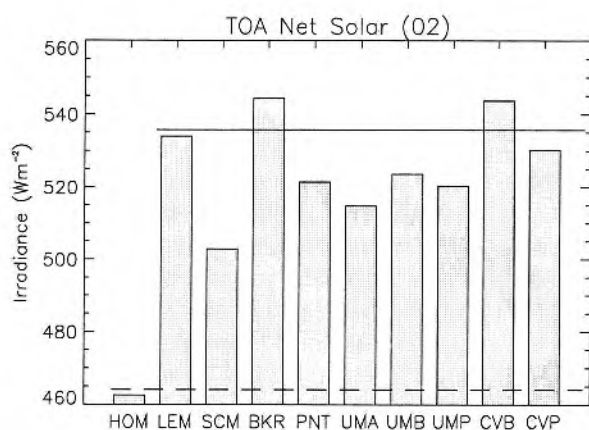


Figure 4: Infra-red (upper) and solar (lower) heating rates from days 2 (S02), 3 (S03) and 5 (S05). Shown are results from the 3-D LEM, from single column calculations [SCM] and from the 3-D LEM using homogeneous cloud [HOM].





KEY:

HOM - Averaged radiation using homogenized cloud
 LEM - Averaged radiation from standard LEM dataset
 SCM - Standard column calculation using domain average
 BKR - Barker (1996) type correction to SCM
 PNT - Point 7(Tiedke, 1996) correction to SCM
 UMA - SCM calculation using 2 cloud types
 UMB - Barker (1996) correction to large scale cloud
 UMP - Point 7 correction to large scale cloud
 CVB - as UMB with Point 5 convective correction
 CVP - Point 7 correction to both cloud types

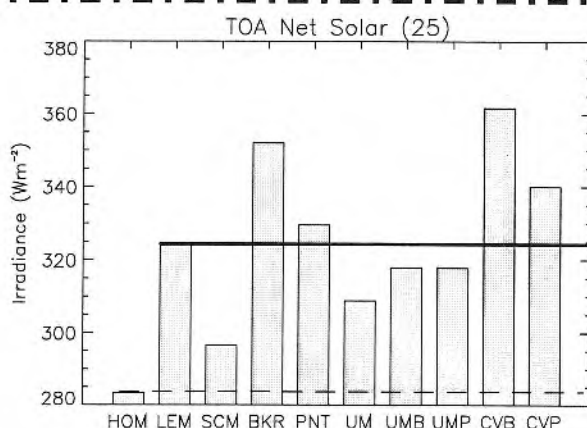
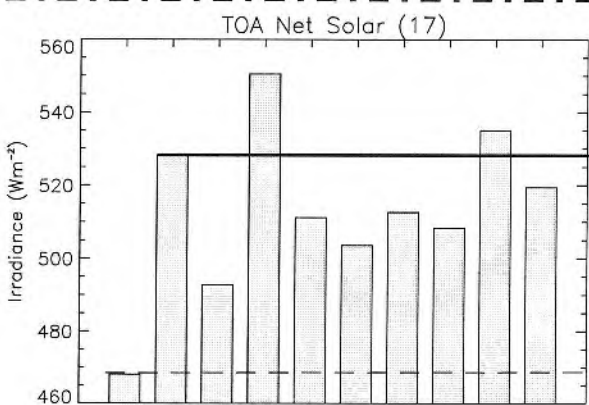
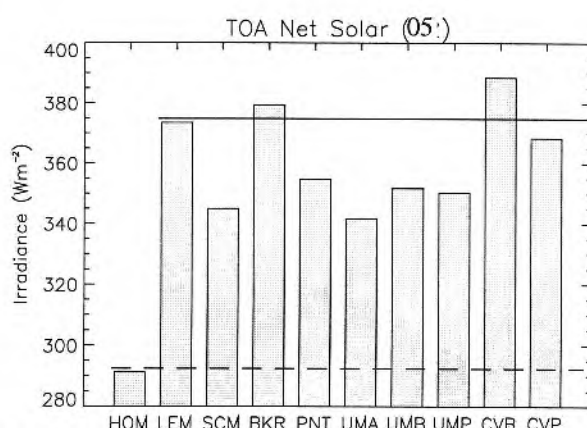
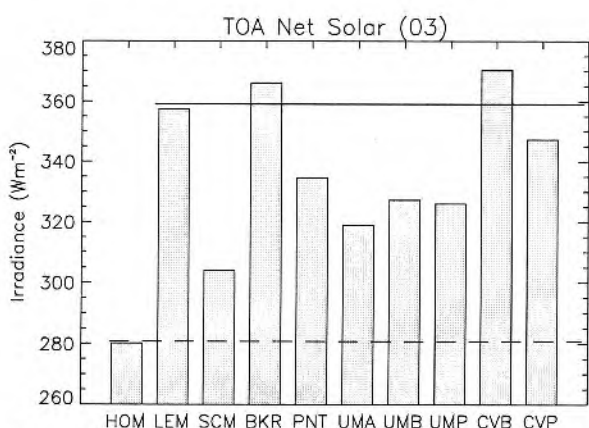
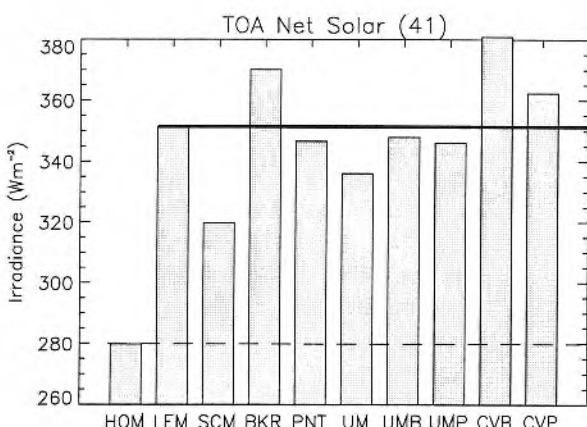


Figure 6: TOA net downward radiation from days 2, 3 and 5 of the 3-D (top) and 2-D (bottom) LEM simulations. Shown are results from the LEM (LEM; solid line), the LEM using homogeneous cloud (HOM; dashed line) and all the single column calculations described in this paper (see KEY).



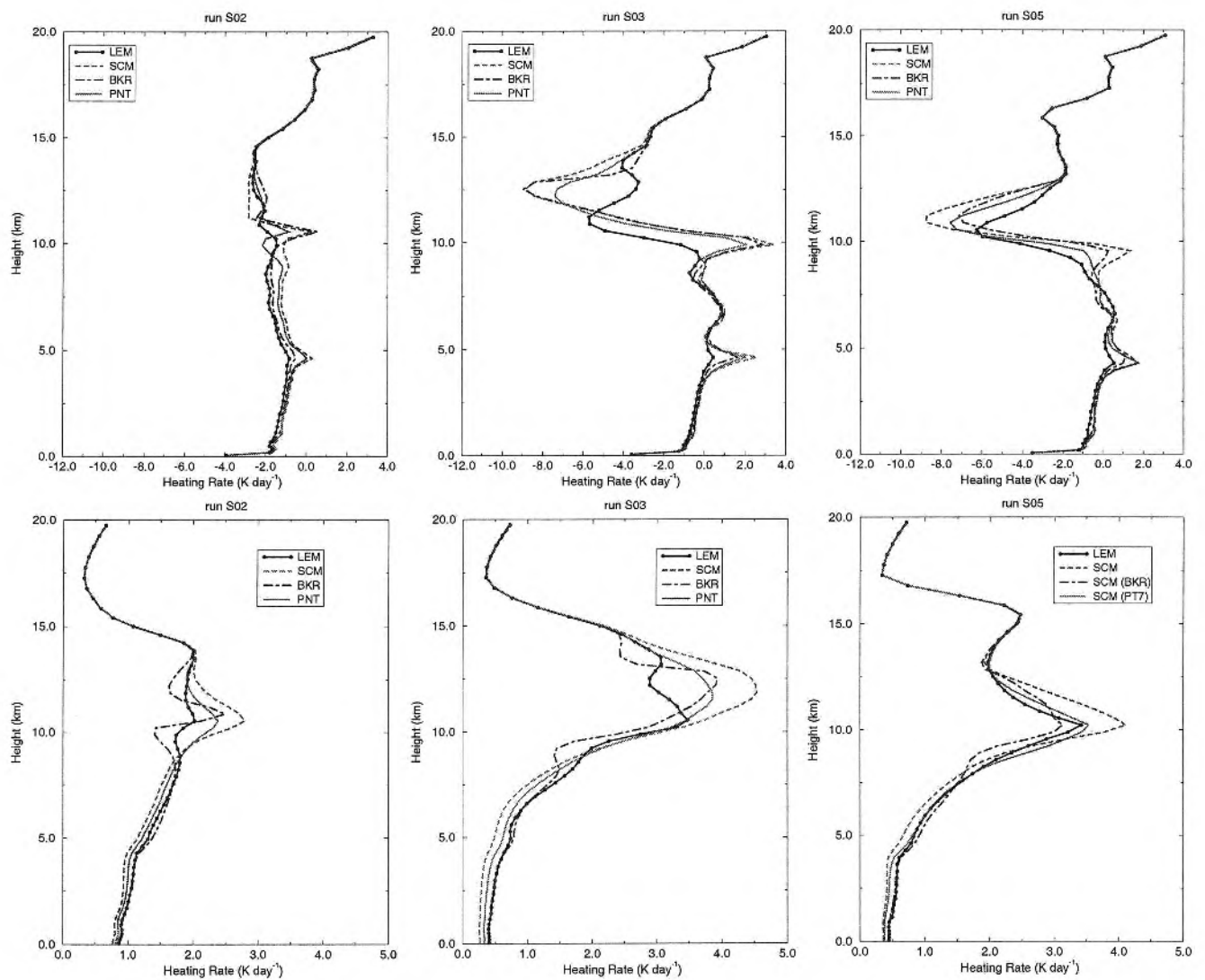


Figure 7: Infra-red (upper) and solar (lower) heating rates from days 2, 3 and 5 from the 3-D LEM simulation. Shown are results from the LEM, and from single column calculations without [SCM] and with two inhomogeneity parametrizations (Barker [BKR] and Point 7 [PNT]).

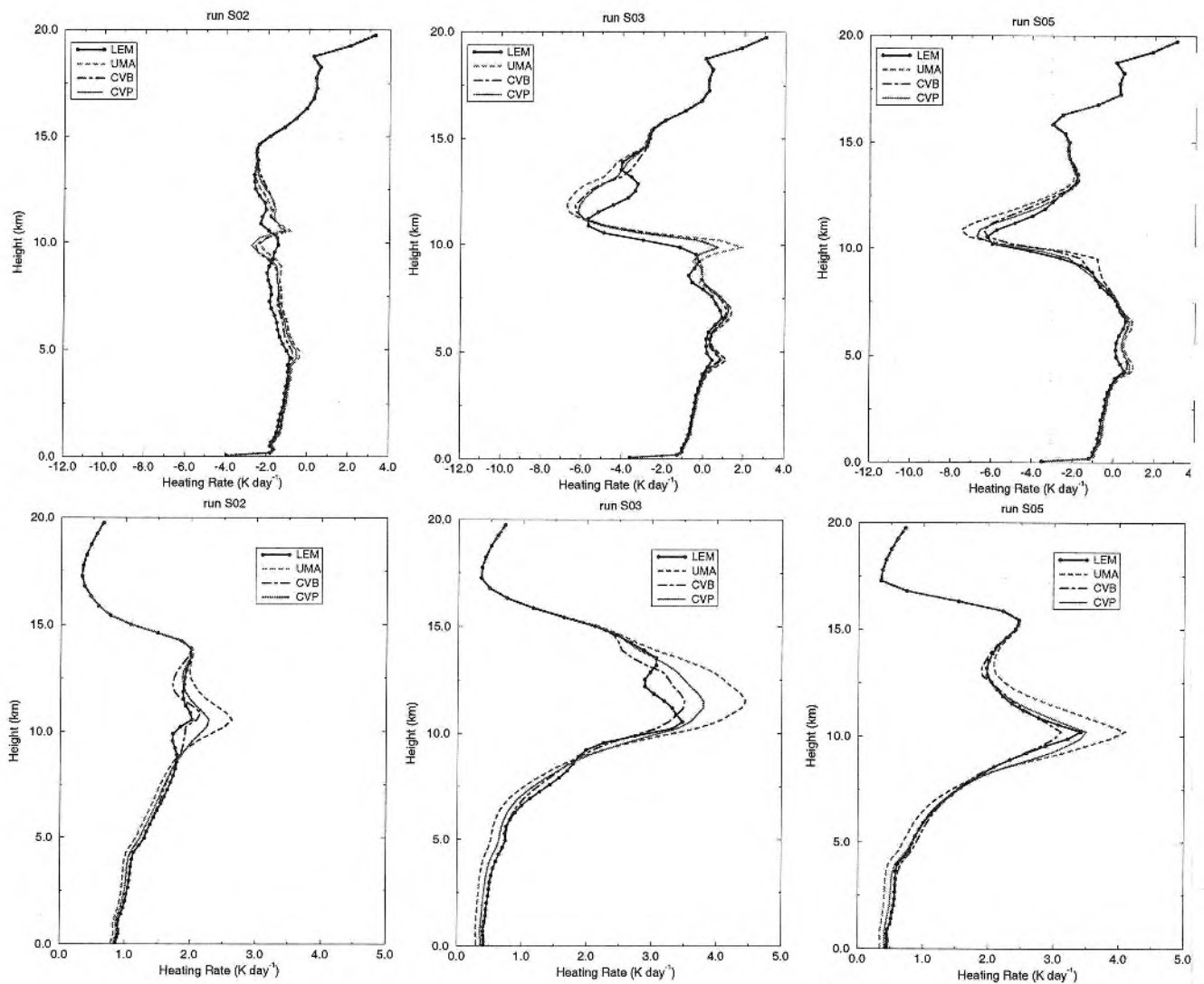


Figure 8: Infra-red (upper) and solar (lower) heating rates from days 2, 3 and 5 from the 3-D LEM simulation. Shown are results from the LEM, and from UMA type single column calculations without [UM] and with two inhomogeneity parametrizations applied to both cloud types (Barker [CVB] and a Point 7 [CVP]).

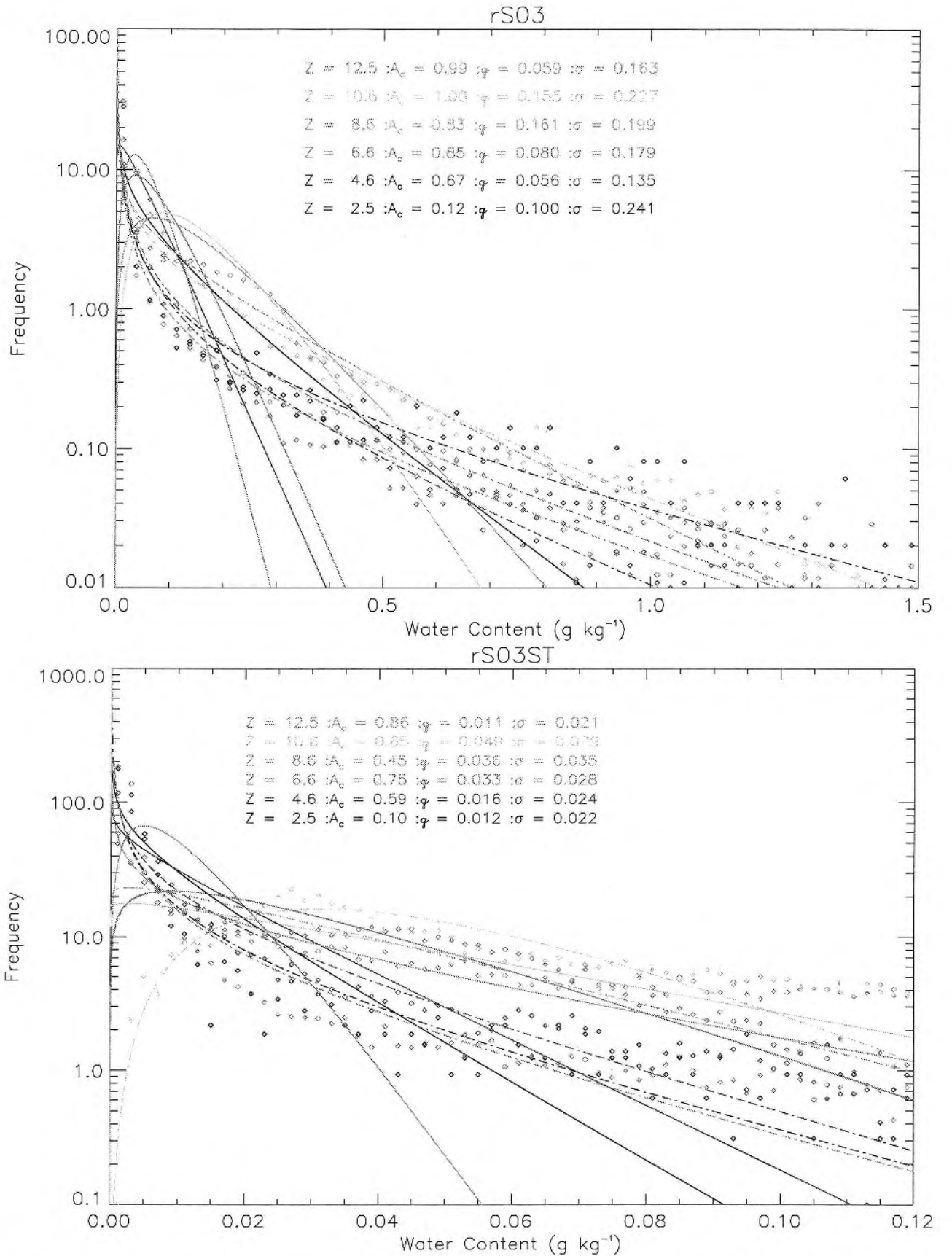


Figure 9: Normalized distribution of cloud water and ice contents from the LEM for day 3 at various heights, z (km), averaged over 1 km in the vertical. The top plot shows the distribution for all clouds and the bottom plot shows the distribution for large scale clouds only. The lines are the modified gamma distribution using the observed standard deviation, σ , [dashed line] and the standard deviation calculated from the cloud fraction [solid line] (Barker, 1996).